Journal of Organometallic Chemistry, 383 (1990) 463–480
Elsevier Sequoia S.A., Lausanne – Printed in The Netherlands
JOM 20195

Ruthenium-platinum carbonyl cluster complexes with bridging methylene, methylidyne, and carbido ligands; crystal structures of the compounds $[Ru_2Pt(\mu\text{-}CH_2)(\mu\text{-}CO)(CO)_2\{P(cyclo\text{-}C_6H_{11})_3\}(\eta\text{-}C_5H_5)_2]$, $[Ru_2Pt_2(\mu\text{-}H)(\mu_4\text{-}CH)(\mu\text{-}CO)(CO)_2(PPr^i_3)_2(\eta\text{-}C_5H_5)_2]$, and $[Ru_2Pt_2(\mu\text{-}H)_2(\mu_4\text{-}C)(\mu\text{-}CO)_2(PPr^i_3)_2(\eta\text{-}C_5H_5)_2]$

David L. Davies, John C. Jeffery, Daniel Miguel, Paul Sherwood, and F. Gordon A. Stone *

Department of Inorganic Chemistry, The University of Bristol, Bristol BS8 1TS (Great Britain)

(Received April 18th, 1989)

Abstract

The diruthenium compounds $[Ru_2(\mu\text{-}CH_2)(\mu\text{-}CO)(CO)(L)(\eta\text{-}C_5H_5)_2]$ (L = CO or NCMe) react under mild conditions with the platinum reagents $[Pt(C_2H_4)_2(PR_3)]$ (R = cyclo-C_6H_{11} or Pr^i) to give tri- and tetra-nuclear cluster compounds $[Ru_2Pt(\mu\text{-}CH_2)(\mu\text{-}CO)(CO)_2(PR_3)(\eta\text{-}C_5H_5)_2]$, $[Ru_2Pt_2(\mu\text{-}H)(\mu_4\text{-}CH)(\mu\text{-}CO)(CO)_2(PR_3)_2(\eta\text{-}C_5H_5)_2]$, and $[Ru_2Pt_2(\mu\text{-}H)_2(\mu_4\text{-}C)(\mu\text{-}CO)_2(PR_3)_2(\eta\text{-}C_5H_5)_2]$. The structures of the complexes $[Ru_2Pt(\mu\text{-}CH_2)(\mu\text{-}CO)(CO)_2\{P(cyclo\text{-}C_6H_{11})_3\}(\eta\text{-}C_5H_5)_2]$, $[Ru_2Pt_2(\mu\text{-}H)(\mu_4\text{-}CH)(\mu\text{-}CO)(CO)_2(PPr^i_3)_2(\eta\text{-}C_5H_5)_2]$, and $[Ru_2Pt_2(\mu\text{-}H)_2(\mu_4\text{-}C)(\mu\text{-}CO)_2(PPr^i_3)_2(\eta\text{-}C_5H_5)_2]$ have been established by X-ray diffraction. The first compound has a structure based on an Ru_2Pt triangle, with one Ru–Pt bond bridged by a methylene group and the other by a carbonyl ligand. The Ru–Ru–Pt–Pt ring in the second complex has a CO group bridging the Pt–Pt bond and a hydrido ligand bridging one of the two Ru–Pt bonds. The ring is capped by the CH group; the first example of this mode of bonding for a methylidyne fragment in a metal cluster. The carbido complex has a Ru–Pt–Ru–Pt metal core which is folded about the two platinum atoms, but the separation of these atoms (3.132(1) Å) suggests little or no direct metal–metal bonding. The Ru–C–Ru arrangement is nearly linear (175.4(5)°). Each Ru–Pt bond in the metal ring is alternately bridged either by a carbonyl or a hydrido ligand. The NMR spectra (^1H, $^{13}C\text{-}\{^1H\}$, $^{31}P\text{-}\{^1H\}$, or $^{195}Pt\text{-}\{^1H\}$) of the new complexes are reported and discussed.

The discovery [1] of the compounds $[Pt(cod)_2]$ (cod = cycloocta-1,5-diene), $[Pt(C_2H_4)_3]$, and $[Pt(C_2H_4)_2(PR_3)]$ (R = alkyl or aryl) opened the way to the

0022-328X/90/$03.50 © 1990 Elsevier Sequoia S.A.

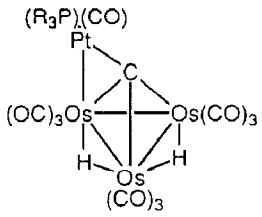

I

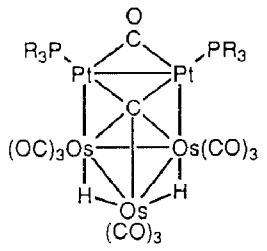

II

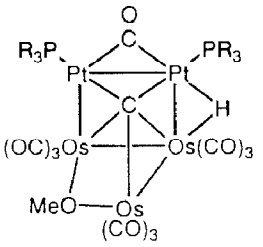

III

R = cyclo-C_6H_{11}

synthesis of a variety of 'mixed-metal' carbonyls containing platinum bonded to other transition elements [2]. The platinum reagents readily react either with electronically saturated or with unsaturated metal carbonyl complexes with incorporation of Pt atoms or $Pt(PR_3)$ fragments into the metal core of the clusters produced. Representative examples of such syntheses include those of $[Os_3Pt(\mu\text{-}H)_2(CO)_{10}\{P(\text{cyclo-}C_6H_{11})_3\}]$ [3a], $[N(PPh_3)_2][Fe_2Pt_2(\mu\text{-}H)(\mu\text{-}CO)_3(CO)_5(PPh_3)_2]$ [3b], $[Os_2Pt_2(\mu\text{-}H)_2(CO)_8(PPh_3)_2]$ [3c], $[Re_2Pt(\mu\text{-}H)_2(CO)_9(PPh_3)]$ [4], $[Rh_4Pt(\mu\text{-}CO)_4(\eta\text{-}C_5Me_5)_4]$ [5], $[Ir_3Pt_3(\mu\text{-}CO)_3(CO)_3(\eta\text{-}C_5Me_5)_3]$ [6], and $[W_4Pt_4(\mu\text{-}CC_6H_4Me\text{-}4)(\mu_3\text{-}CC_6H_4Me\text{-}4)_3(\mu\text{-}CO)(CO)_7(\eta\text{-}C_5H_5)_4]$ [7].

Some years after we first introduced this methodology [8], we investigated the reaction between the methylidyne compound $[Os_3(\mu\text{-}H)(\mu_3\text{-}CH)(CO)_{10}]$ and $[Pt(C_2H_4)_2\{P(\text{cyclo-}C_6H_{11})_3\}]$, with the object of preparing an Os_3Pt carbonyl cluster containing a bridging CH ligand [9]. However, the reaction did not afford the anticipated μ-methylidyne triosmium-platinum complex, but instead yielded two 'mixed-metal' carbido-carbonyl clusters $[Os_3Pt(\mu\text{-}H)_2(\mu_4\text{-}C)(CO)_{10}\{P(\text{cyclo-}C_6H_{11})_3\}]$ (I) and $[Os_3Pt_2(\mu\text{-}H)_2(\mu_5\text{-}C)(\mu\text{-}CO)(CO)_9\{P(\text{cyclo-}C_6H_{11})_3\}_2]$ (II). Moreover, it was also found that the methoxymethylidyne complex $[Os_3(\mu\text{-}H)(\mu\text{-}COMe)(CO)_{10}]$ reacted with the platinum reagent to yield a carbido-carbonyl compound $[Pt_2Os_3(\mu\text{-}H)(\mu_5\text{-}C)(\mu\text{-}OMe)(\mu\text{-}CO)(CO)_9\{P(\text{cyclo-}C_6H_{11})_3\}_2]$ (III).

Carbido-carbonyl metal cluster compounds are well established species [10,11]. Indeed, the first complex of this type to be discovered $[Fe_5(\mu_5\text{-}C)(CO)_{15}]$ was structurally characterised by X-ray diffraction over twenty years ago [12]. Several of the known homopolynuclear metal-carbido compounds result from heating carbonyls of low metal nuclearity in high boiling solvents, under which condition it is believed that two CO ligands combine to give a μ-C group, with release of a molecule of

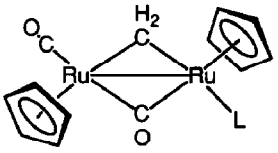

IVa L = CO
IVb L = NCMe

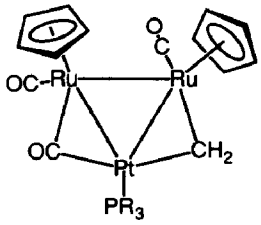

Va R = cyclo-C_6H_{11}
Vb R = Pr^i

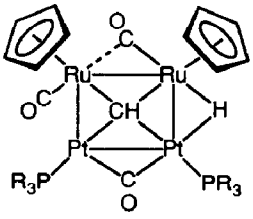

VIa R = cyclo-C_6H_{11}
VIb R = Pr^i

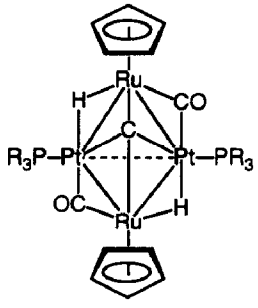

VIIa R = cyclo-C_6H_{11}
VIIb R = Pr^i

CO_2. In more recent times the synthesis of 'mixed-metal' carbido-carbonyl clusters has been addressed, and species of this kind have been obtained via two routes. Anionic homopolynuclear metal species such as $[Fe_5(\mu_5\text{-}C)(CO)_{14}]^{2-}$ or $[Ru_6(\mu_6\text{-}C)(CO)_{16}]^{2-}$ react with a variety of transition metal complexes containing labile ligands, affording either anionic or neutral heteronuclear metal-carbido clusters, e.g. $[Fe_5Ir(\mu_6\text{-}C)(CO)_{14}(cod)]^-$ [13] or $[Ru_6Cu_2(\mu_6\text{-}C)(CO)_{16}(NCMe)_2]$ [14]. Alternatively, treatment of the ketenylidene triiron cluster $[N(PPh_3)_2]_2[Fe_3(\mu_3\text{-}CCO)(CO)_9]$ with certain electrophilic transition metal reagents gives a range of mixed-metal carbido carbonyl compounds, e.g. $[N(PPh_3)_2]_2[WFe_3(\mu_4\text{-}C)(CO)_{13}]$ or $[N(PPh_3)_2][Fe_3Rh_3(\mu_6\text{-}C)(CO)_{15}]$ [15].

The syntheses employing $[N(PPh_3)_2]_2[Fe_3(\mu_3\text{-}CCO)(CO)_9]$ are relevant to the preparation of the compounds I and II since these species can also be obtained by treating the ketenylidene complex $[Os_3(\mu\text{-}H)_2(\mu_3\text{-}CCO)(CO)_9]$ with $[Pt(C_2H_4)_2\{P(cyclo\text{-}C_6H_{11})_3\}]$ [9]. Indeed, $[Os_3(\mu\text{-}H)(\mu_3\text{-}CH)(CO)_{10}]$ is a tautomer of $[Os_3(\mu\text{-}H)_2(\mu_3\text{-}CCO)(CO)_9]$ and so in using the former as a reagent for preparing I and II, it is possible that the latter is an intermediate. Nevertheless, the reactions leading to compounds I–III show that the μ-CX (X = H, CO or OMe) groups present in the triosmium carbonyl complexes can be transformed into μ-C ligands as a result of attack by the nucleophilic $Pt\{P(cyclo\text{-}C_6H_{11})_3\}$ fragment. This represents an interesting synthetic route to heteropolynuclear metal carbido-carbonyl compounds, and one which may be capable of extension to other systems.

In this paper we report reactions between the diruthenium compounds $[Ru_2(\mu\text{-}CH_2)(\mu\text{-}CO)(CO)(L)(\eta\text{-}C_5H_5)_2]$ (L = CO (IVa) or NCMe (IVb)) and the platinum reagents $[Pt(C_2H_4)_2(PR_3)]$ (R = cyclo-C_6H_{11} or Pr^i). These studies were carried out

Table 1

Analytical and other data

Compound	Colour	Yield (%)	ν_{max}(CO) (cm^{-1})	Analysis (Found (calcd) (%))	
				C	H
$[Ru_2Pt(\mu\text{-}CH_2)(\mu\text{-}CO)(CO)_2\{P(cyclo\text{-}C_6H_{11})_3\}(\eta\text{-}C_5H_5)_2]$ (Va)	Purple	69	[a] 1934w, 1913s, 1799m	42.6 (42.4)	5.0 (5.0)
$[Ru_2Pt(\mu\text{-}CH_2)(\mu\text{-}CO)(CO)_2(PPr^i_3)(\eta\text{-}C_5H_5)_2]$ (Vb)	Purple	67	[a] 1936w, 1914s, 1800m	34.8 (35.2)	4.2 (4.2)
$[Ru_2Pt_2(\mu\text{-}H)(\mu_4\text{-}CH)(\mu\text{-}CO)(CO)_2\{P(cyclo\text{-}C_6H_{11})_3\}_2(\eta\text{-}C_5H_5)_2]$ (VIa)	Yellow-orange	5	[b] 1909s, 1796(sh), 1762s	43.2 (43.5)	5.3 (5.7)
$[Ru_2Pt_2(\mu\text{-}H)(\mu_4\text{-}CH)(\mu\text{-}CO)(CO)_2(PPr^i_3)_2(\eta\text{-}C_5H_5)_2]$ (VIb)	Yellow	7	[b] 1910s, 1795(sh), 1756s	33.4 (33.7)	4.8 (4.8)
$[Ru_2Pt_2(\mu\text{-}H)_2(\mu_4\text{-}C)(\mu\text{-}CO)_2\{P(cyclo\text{-}C_6H_{11})_3\}_2(\eta\text{-}C_5H_5)_2]$ (VIIa)	Yellow	45	[c] 1777w, 1767s	43.9 (44.0)	6.2 (5.8)
$[Ru_2Pt_2(\mu\text{-}H)_2(\mu_4\text{-}C)(\mu\text{-}CO)_2(PPr^i_3)_2(\eta\text{-}C_5H_5)_2]$ (VIIb)	Yellow	41	[c] 1780w, 1770s	33.6 (33.5)	5.0 (4.9)

[a] In Et_2O. [b] In CH_2Cl_2. [c] In light petroleum.

to establish whether $Pt(PR_3)$ fragments would add to the diruthenium species to afford cluster compounds, and whether in the products methylidyne or carbido ligands would be formed by degradation of the μ-methylene ligands in IV [16].

Results and discussion

Treatment of a diethyl ether solution of IVa with $[Pt(C_2H_4)_2\{P(cyclo\text{-}C_6H_{11})_3\}]$ in the same solvent at room temperature afforded a mixture of the purple crystalline complex $[Ru_2Pt(\mu\text{-}CH_2)(\mu\text{-}CO)(CO)_2\{P(cyclo\text{-}C_6H_{11})_3\}(\eta\text{-}C_5H_5)_2]$ (Va) (ca. 70%), and the yellow orange crystalline complex $[Ru_2Pt_2(\mu\text{-}H)(\mu_4\text{-}CH)(\mu\text{-}CO)(CO)_2\{P(cyclo\text{-}C_6H_{11})_3\}_2(\eta\text{-}C_5H_5)_2]$ (VIa) (ca. 5%). The two products were readily separated by column chromatography on alumina. A similar reaction between $[Pt(C_2H_4)_2(PPr^i_3)]$ and IVa gave the two compounds $[Ru_2Pt(\mu\text{-}CH_2)(\mu\text{-}CO)(CO)_2(PPr^i_3)(\eta\text{-}C_5H_5)_2]$ (Vb) and $[Ru_2Pt_2(\mu\text{-}H)(\mu_4\text{-}CH)(\mu\text{-}CO)(CO)_2(PPr^i_3)_2(\eta\text{-}C_5H_5)_2]$ (VIb). Data characterising complexes V and VI are listed in Tables 1 and 2, but discussion of the spectroscopic properties is deferred until the results of single-crystal X-ray diffraction studies on compounds Va and VIb are described.

The molecular structure of Va is shown in Fig. 1, and selected inter-atomic distances are listed in Table 3. The core of the molecule consists of a triangle of metal atoms (Ru(1)–Ru(2) 2.813(2), Ru(1)–Pt 2.609(1), Ru(2)–Pt 2.613(1) Å) with one of the Ru–Pt edges bridged by a CO ligand (Ru–C(2)–O(2) 132(1), Pt–C(2)–O(2) 148°), and the other by a CH_2 group (Ru(1)–C(1) 2.07(1), Pt–C(1) 2.05(1) Å). The platinum atom carries the phosphine ligand (Pt–P 2.288(3) Å), as expected, and each ruthenium atom is ligated by a terminal CO group and a C_5H_5 ring. The two C_5H_5 and the two CO ligands are, respectively, transoid to each other about the Ru–Ru bond. The latter is similar in length to the two metal–metal linkages in the triruthenium compound $[Ru_3(CO)_8(\eta\text{-}C_5H_5)_2]$ (2.889(1) Å) which has a linear array of three metal atoms with no bridging ligands [17]. In contrast, the Ru–Ru separations are shorter in the precursor IVa (2.707(1) Å) and in other related diruthenium compounds with bridging groups [18]. This is in accord with the general property that metal–metal bonds which have bridging ligands are shorter than those that are not bridged, unless a μ-H group is involved, in which case the trend is reversed.

The Ru–Pt distances in Va are appreciably shorter than those found for such connectivities (range 2.707–2.858 Å) in other ruthenium–platinum clusters in which the metal–metal bonds are also spanned by bridging groups [19,20]. The μ-CH_2 and μ-CO ligands in Va bridge their respective Ru–Pt bonds in an essentially symmetrical manner.

The molecular structure of VIb is shown in Fig. 2, and selected internuclear distances and angles are given in Table 4. The novelty of the structure, with its CH fragment bridging a ring of four metal atoms, is immediately apparent. The Ru(1)–Ru(2) distance (2.809(1) Å) is very similar to the corresponding distance in Va. The Ru(1)–Pt(2) separation (2.820(1) Å) is perceptibly longer than Ru(2)–Pt(1) (2.803(1) Å), as expected, since the former is bridged by the hydrido ligand. The latter was located in a final electron density difference map, and its presence was clearly revealed by NMR data discussed below. The Pt–Pt vector (2.662(1) Å) is bridged by a CO ligand (Pt–C–O ca. 139°). Like VIb, the complex $[RuPt_2(\mu\text{-}$

Table 2

^{1}H, ^{13}C-{^{1}H}, ^{31}P-{^{1}H}, and ^{195}Pt-{^{1}H} NMR data [a]

Compound	$\delta(^{1}H)$ [b]	$\delta(^{13}C)$ [c,d]	$\delta(^{31}P)$ [b,e]	$\delta(^{195}Pt)$ [b,f]
Va	1.30–2.20 (m, 33 H, C_6H_{11}), 5.19, 5.18 (s×2, 10 H, C_5H_5), 7.85 [br, 2 H, CH_2, J(PtH) 18]	244.1 [d, μ-CO, J(PC) 5, J(PtC) 858], 208.3 [CO, J(PtC) 49], 142.8 [μ-CH_2, J(PtC) 576], 86.3, 86.1 (C_5H_5), 35.0–27.0 (C_6H_{11})	59.7 [J(PtP) 3433]	794.4 [d, J(PPt) 3433]
Vb	0.99–1.22 (m, 18 H, Me), 2.20–2.61 (m, 3 H, CH), 5.18, 5.20 (s×2, 10 H, C_5H_5), 7.93 (br m, 2 H, CH_2, J(PtH) 18]	244.5 (μ-CO), 208.4 [CO, J(PtC) 46] 142.9 [μ-CH_2, J(PtC) 573], 86.4, 86.1 (C_5H_5), 26.4–19.5 ($CHMe_2$)	71.1 [J(PtP) 3462]	770.5 [d, J(PPt) 3462]
VIa	−12.61 [d of d, 1 H, μ-H, J(PH) 14 and 4, J(PtH) 627 and 75], 1.20–2.20 (m, 66 H, C_6H_{11}), 5.06, 5.12 (s×2, 10 H, C_5H_5), 14.87 [d of d, 1 H, μ_4-CH, J(PH) 6, 2, J(PtH) 60, 25]	248.9 [d of d, μ_4-CH, J(PC) 45 and 36], 235.5 (μ-CO), 223.0 (RuCO), 202.9 [RuCO, J(PtC) 76], 89.4, 83.3 (C_5H_5), 36.0–26.9 (C_6H_{11})	44.8 [d, J(PP) 12, J(PtP) 5659 and 342] 25.7 [d, J(PP) 12, J(PtP) 3964 and 281]	330.5 [d of d, J(PPt) 5659 and 281, J(PtPt) 2080] 572.7 [d of d, J(PPt) 3964 and 342, J(PtPt) 2080]
VIb	−12.51 [d of d, 1 H, μ-H, J(PH) 14 and 4, J(PtH) 622 and 74], 0.89–1.50 (m, 36 H, Me), 2.38–2.56 (m, 6 H, CH), 5.07, 5.10 (s×2, 10 H, C_5H_5), 14.89 [d of d, 1 H, μ_4-CH, J(PH) 6 and 2, J(PtH) 56 and 22]	248.1 [d of d, μ_4-CH, J(PC) 44 and 35, J(PtC) 262 and 192], 236.2 [μ-CO, J(PtC) 1087 and 1011], 221.0 (RuCO), 201.8 [RuCO, J(PtC) 74], 84.8, 83.0 (C_5H_5), 26.2–19.2 ($CHMe_2$)	54.5 [d, J(PP) 12, J(PtP) 5650 and 347] 36.9 [d, J(PP) 12, J(PtP) 4023 and 287]	298.6 [d of d, J(PPt) 5650 and 287, J(PtPt) 2075] 588.2 [d of d, J(PPt) 4023 and 347, J(PtPt) 2075]
VIIa	−13.00 [d, 2 H, μ-H, J(PH) 15, J(PtH) 604 and 23], 1.21–1.73 (m br, 66 H, C_6H_{11}), 5.19 (s, 10 H, C_5H_5)	438.9 (μ_4-C), 250.2 (μ-CO), 85.2 (C_5H_5), 36.0–26.8 (C_6H_{11})	30.4 [J(PtP) 5186]	−723.9 [d, J(PtP) 5186]
VIIb	−12.89 [d, 2 H, μ-H, J(PH) 15, J(PtH) 609 and 23], 0.90–1.18 (m, 36 H, Me), 2.11–2.54 (m, 6 H, CH), 5.20 (s, 10 H, C_5H_5)	439.5 [t, μ_4-C, J(PC) 23, J(PtC) 104], 250.3 [μ-CO, J(PtC) 1002], 85.3 (C_5H_5), 26.4–24.7 (m, CH), 20.3–19.4 (m, Me)	41.9 [J(PtP) 5227]	−763.4 [d, J(PtP) 5227, J(PtPt) 365]

[a] Chemical shifts (δ) in ppm, coupling constants in Hz. Measurements at room temperature. [b] Measured in $CDCl_3$. [c] Measured in CD_2Cl_2/CH_2Cl_2. [d] Hydrogen-1 decoupled, chemical shifts are positive to high frequency of $SiMe_4$ (0.0 ppm). [e] Hydrogen-1 decoupled, chemical shifts are positive to high frequency of 85% H_3PO_4 (external) (0.0 ppm). [f] Hydrogen-1 decoupled, chemical shifts are positive to high frequency of $\Xi(^{195}Pt)$ 21.4 MHz.

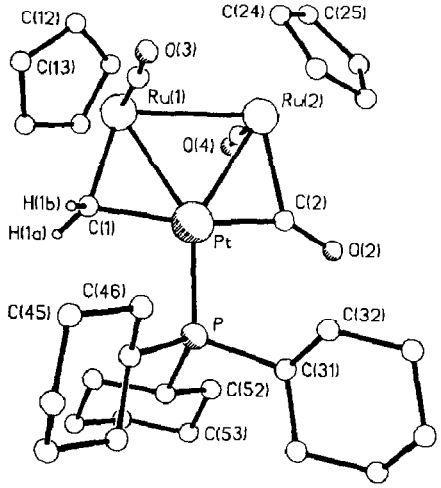

Fig. 1. The molecular structure of $[Ru_2Pt(\mu\text{-}CH_2)(\mu\text{-}CO)(CO)_2\{P(cyclo\text{-}C_6H_{11})_3(\eta\text{-}C_5H_5)_2]$ (Va) showing the crystallographic numbering scheme.

$CO)_3(CO)_2(PMePh_2)_3]$ also contains a $R_3PPt(\mu\text{-}CO)PtPR_3$ fragment and the Pt–Pt distance (2.647(2) Å) is very similar [19,20].

Although VIb, like Va, contains an $Ru_2(CO)_2(\eta\text{-}C_5H_5)_2$ unit the disposition of the ligands about the Ru–Ru bond is different. In VIb the C_5H_5 rings adopt a cisoid arrangement, and although C(3)O(3) is essentially terminally bound to Ru(2),

Table 3

Selected internuclear distances (Å) and angles (°) for $[Ru_2Pt(\mu\text{-}CH_2)(\mu\text{-}CO)(CO)_2\{P(C_6H_{11})_3\}(\eta\text{-}C_5H_5)_2]$ (Va), with estimated standard deviations in parentheses

Pt–Ru(1)	2.609(1)	Pt–Ru(2)	2.613(1)
Pt–P	2.288(3)	Pt–C(1)	2.05(1)
Pt–C(2)	1.94(1)	Ru(1)–Ru(2)	2.813(2)
Ru(1)–C(1)	2.07(1)	Ru(1)–C(3)	1.80(1)
Ru(2)–C(2)	2.10(1)	Ru(2)–C(4)	1.85(1)
C(2)–O(2)	1.20(1)	C(3)–O(3)	1.18(1)
C(4)–O(4)	1.16(1)		
Ru(1)–Pt–Ru(2)	65.2(1)	Ru(1)–Pt–P	145.9(1)
Ru(2)–Pt–P	148.4(1)	Ru(1)–Pt–C(1)	51.0(3)
Ru(2)–Pt–C(1)	94.9(4)	P–Pt–C(1)	94.9(4)
Ru(1)–Pt–C(2)	116.3(3)	Ru(2)–Pt–C(2)	52.6(3)
P–Pt–C(2)	97.6(3)	C(1)–Pt–C(2)	166.6(5)
Pt–Ru(1)–Ru(2)	57.5(1)	Pt–Ru(1)–C(1)	50.4(3)
Ru(2)–Ru(1)–C(1)	107.6(3)	Pt–Ru(1)–C(3)	88.6(3)
Ru(2)–Ru(1)–C(3)	84.2(4)	C(1)–Ru(1)–C(3)	88.1(5)
Pt–Ru(2)–Ru(1)	57.3(1)	Pt–Ru(2)–C(2)	47.0(3)
Ru(1)–Ru(2)–C(2)	103.2(3)	Pt–Ru(2)–C(4)	93.2(4)
Ru(1)–Ru(2)–C(4)	86.3(4)	C(2)–Ru(2)–C(4)	86.6(5)
Pt–C(1)–Ru(1)	78.5(4)	Pt–C(2)–Ru(2)	80.4(4)
Pt–C(2)–O(2)	148(1)	Ru(2)–C(2)–O(2)	132(1)
Ru(1)–C(3)–O(3)	175(1)	Ru(2)–C(4)–O(4)	175(1)

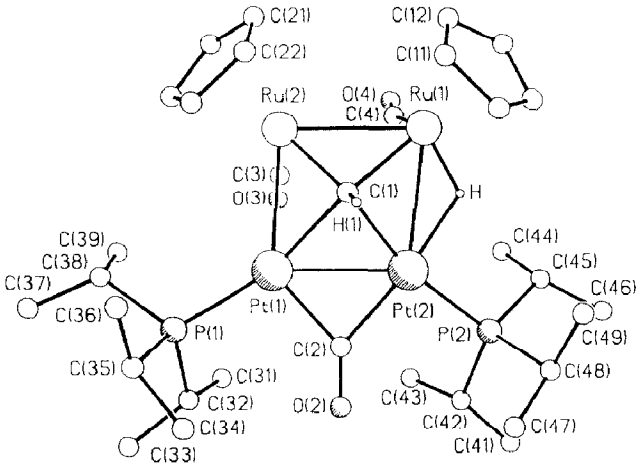

Fig. 2. The molecular structure of $[Ru_2Pt_2(\mu\text{-}H)(\mu_4\text{-}CH)(\mu\text{-}CO)(CO)_2(PPr^i_3)_2(\eta\text{-}C_5H_5)_2]$ (VIb) showing the crystallographic numbering scheme.

the C(4)O(4) group semi-bridges the Ru–Ru bond (Ru(1)–C(4)–O(4) 163(2)°). The P(cyclo-C_6H_{11})$_3$ groups ligate the Pt atoms, as expected.

Interest centres on the μ_4-CH ligand which spans the metal ring with C–M (Ru or Pt) distances in the range 2.07–2.18 Å. The ring is non-planar (Fig. 3), with Pt(1) deviating by 0.594 Å from the plane defined by Pt(2), Ru(1), and Ru(2). The torsion angle P(1)–Pt(1)–Pt(2)–P(2) is 8.8°. The hydrogen atom of the CH group was located in the X-ray study, and its presence was clearly revealed in the NMR spectra discussed below. Although the H(1)–C(1)–M (Ru or Pt) angles have large e.s.d.'s, and are thus imprecise, it is evident that the C–H bond points away from the ring of four metal atoms. There is thus an analogy with a C(1) fragment located on the fourfold symmetry axis of the (100) surface plane of a body-centred cubic metal. The structure is to our knowledge unique, and contrasts with that of $[Fe_4(\mu\text{-}H)(\mu_4\text{-}CH)(CO)_{12}]$ which has an agostic C–H→Fe interaction with the Fe_4 core adopting a butterfly configuration [21]. In the iron compound the C–H fragment formally contributes five electrons to a 62 valence electron cluster, whereas in VIb the C–H group contributes three electrons to a 60 valence electron cluster.

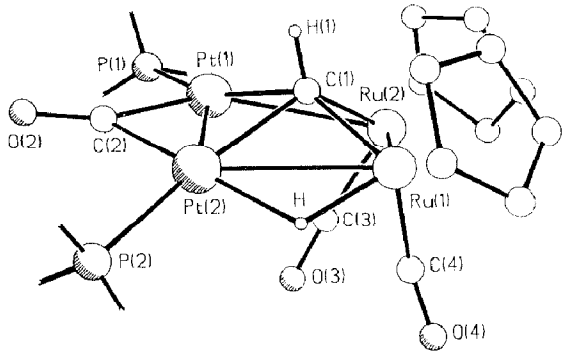

Fig. 3. Molecular structure of VIb showing the geometry of the μ_4-CRu_2Pt_2 core. The Pr^i substituents of P(1) and P(2) have been omitted for clarity.

Table 4

Selected internuclear distances (Å) and angles (°) for $[Ru_2Pt_2(\mu\text{-H})(\mu_4\text{-CH})(\mu\text{-CO})(CO)_2(PPr^i_3)_2(\eta\text{-}C_5H_5)_2]$ (VIb), with estimated standard deviations in parentheses

Pt(1)–Pt(2)	2.662(1)	Pt(1)–Ru(2)	2.803(1)
Pt(1)–P(1)	2.248(3)	Pt(1)–C(1)	2.18(1)
Pt(1)–C(2)	2.003(9)	Pt(2)–Ru(1)	2.820(1)
Pt(2)–H	1.9(1)	Pt(2)–P(2)	2.275(2)
Pt(2)–C(1)	2.122(8)	Pt(2)–C(2)	2.04(1)
Ru(1)–Ru(2)	2.809(1)	Ru(1)–H	1.60(9)
Ru(1)–C(1)	2.07(2)	Ru(1)–C(4)	1.83(2)
Ru(2)–C(1)	2.04(1)	Ru(2)–C(3)	1.86(1)
C(1)–H(1)	1.0(1)	C(2)–O(2)	1.15(1)
C(3)–O(3)	1.16(1)	C(4)–O(4)	1.16(3)
Pt(2)–Pt(1)–Ru(2)	85.9(1)	Pt(2)–Pt(1)–P(1)	147.6(1)
Ru(2)–Pt(1)–P(1)	123.2(1)	Pt(2)–Pt(1)–C(1)	50.8(2)
Ru(2)–Pt(1)–C(1)	46.4(3)	P(1)–Pt(1)–C(1)	160.6(2)
Pt(2)–Pt(1)–C(2)	49.5(3)	Ru(2)–Pt(1)–C(2)	135.3(3)
P(1)–Pt(1)–C(2)	99.6(3)	C(1)–Pt(1)–C(2)	95.8(4)
Pt(1)–Pt(2)–Ru(1)	95.6(1)	Pt(1)–Pt(2)–H	127(3)
Ru(1)–Pt(2)–H	33(3)	Pt(1)–Pt(2)–P(2)	141.6(1)
Ru(1)–Pt(2)–P(2)	120.2(1)	H–Pt(2)–P(2)	87(3)
Pt(1)–Pt(2)–C(1)	52.6(3)	Ru(1)–Pt(2)–C(1)	47.1(3)
H–Pt(2)–C(1)	80(3)	P(2)–Pt(2)–C(1)	165.7(3)
Pt(1)–Pt(2)–C(2)	48.2(2)	Ru(1)–Pt(2)–C(2)	142.9(2)
H–Pt(2)–C(2)	175(3)	P(2)–Pt(2)–C(2)	96.9(2)
C(1)–Pt(2)–C(2)	96.3(4)	Pt(2)–Ru(1)–Ru(2)	82.9(1)
Pt(2)–Ru(1)–H	41(4)	Ru(2)–Ru(1)–H	119(4)
Pt(2)–Ru(1)–C(1)	48.5(2)	Ru(2)–Ru(1)–C(1)	46.5(3)
H–Ru(1)–C(1)	89(4)	Pt(2)–Ru(1)–C(4)	94.8(7)
Ru(2)–Ru(1)–C(4)	67.8(5)	H–Ru(1)–C(4)	91(4)
C(1)–Ru(1)–C(4)	102.4(7)	Pt(1)–Ru(2)–Ru(1)	92.7(1)
Pt(1)–Ru(2)–C(1)	50.4(3)	Ru(1)–Ru(2)–C(1)	47.4(3)
Pt(1)–Ru(2)–C(3)	68.7(5)	Ru(1)–Ru(2)–C(3)	97.4(4)
C(1)–Ru(2)–C(3)	97.4(5)	Pt(2)–H–Ru(1)	107(5)
Pt(1)–C(1)–Pt(2)	76.6(3)	Pt(1)–C(1)–Ru(1)	145.8(5)
Pt(2)–C(1)–Ru(1)	84.4(4)	Pt(1)–C(1)–Ru(2)	83.2(4)
Pt(2)–C(1)–Ru(2)	126.8(5)	Ru(1)–C(1)–Ru(2)	86.0(5)
Pt(1)–C(1)–H(1)	107(7)	Pt(2)–C(1)–H(1)	98(5)
Ru(1)–C(1)–H(1)	104(6)	Ru(2)–C(1)–H(1)	135(5)
Pt(1)–C(2)–Pt(2)	82.3(4)	Pt(1)–C(2)–O(2)	138.7(8)
Pt(2)–C(2)–O(2)	139.0(7)	Ru(2)–C(3)–O(3)	174(1)
Ru(1)–C(4)–O(4)	163(2)		

Having established the molecular structures of Va and VIb, the spectroscopic properties of the pairs of compounds V and VI are readily interpretable. Both of the complexes V show three CO stretching bands in their IR spectra, and the absorption at lowest frequency (Va 1799, Vb 1800 cm^{-1}) may be ascribed to the μ-CO ligand. In the ^1H NMR spectra, the resonances of the μ-CH_2 groups (δ 7.85 (Va) and 7.93 (Vb)) occur as broad multiplets with ^{195}Pt-^1H coupling (18 Hz). Resonances in the ^{13}C-$\{^1H\}$ NMR spectra (δ 142.8 (Va) and 142.9 ppm (Vb)) are also diagnostic for the μ-CH_2 ligand. These assignments are confirmed by the association of large ^{195}Pt–^{13}C couplings with these signals (Table 2).

In the IR spectra of the compounds VI there are three CO stretching bands, as expected (Table 1), with the observed frequencies corresponding to terminally bound, semi-bridging, and bridging groups, as found in the X-ray diffraction study on VIb. The NMR spectra (^{1}H, ^{13}C-{^{1}H}, ^{31}P-{^{1}H}, and ^{195}Pt-{^{1}H}) (Table 2) of complexes VIa and VIb are also in agreement with the structure found for VIb in the crystal. The non-equivalent Pt(PR_3) fragments give rise to two ^{31}P and two ^{195}Pt resonances. The ^{1}H spectra show high-field signals (δ −12.61 (VIa) and −12.51 (VIb)) for the μ-H ligands. These occur as a doublet of doublets due to coupling with the non-equivalent PR_3 groups. Moreover, both signals show two sets of ^{195}Pt satellite peaks, as expected.

The ^{1}H and ^{13}C resonances for the μ_4-CH ligand are of interest. The ^{1}H peaks, occur at 14.87 (VIa) and 14.89 ppm (VIb), and each signal shows ^{31}P and ^{195}Pt couplings to the two non-equivalent Pt(PR_3) groups. In the ^{13}C-{^{1}H} NMR spectra resonances of the μ_4-C nuclei occur at δ 248.9 (VIa) and 248.1 ppm (VIb), each signal being a doublet of doublets (J(PC) ca. 35 and 45 Hz). Moreover, the spectrum of VIb was of such quality that two sets of ^{195}Pt satellite peaks (J(PtC) 262 and 192 Hz) were seen, in accord with the presence of the two non-equivalent platinum atoms. In a fully coupled ^{13}C NMR spectrum of VIb the μ_4-C resonance was a doublet (^1J(CH) 140 Hz), confirming the assignment. In this ^{13}C spectrum the peak for the μ-CO ligand at δ 236.2 ppm was also a doublet (^2J(HC) 17 Hz).

The reactions leading to the compounds V revealed that the μ-CH_2 group in IVa can migrate so as to span a Ru–Pt bond in the trimetal species V. Moreover, addition of Pt(PR_3) fragments to the trimetal compounds results in a degradation of the μ-CH_2 ligand to give the μ_4-CH and μ-H groups found in the tetranuclear metal complexes VI. Reactions between the compound [Ru_2(μ-CH_2)(μ-CO)(CO)(NCMe)-(η-C_5H_5)$_2$] (IVb) and the reagents [Pt(C_2H_4)$_2$(PR_3)] (R = cyclo-C_6H_{11} or Pr^i) were next investigated. It was thought, that release of the labile acetonitrile ligand from the diruthenium complex would lead to coordinatively unsaturated metal cluster intermediates, thereby facilitating C–H activation of species containing CH_2 or CH fragments.

Treatment of IVb with the reagents [Pt(C_2H_4)$_2$(PR_3)] gave a mixture of the methylidyne compounds VI and the carbido-carbonyl tetranuclear metal clusters [Ru_2Pt_2(μ-H)$_2$(μ_4-C)(μ-CO)$_2$(PR_3)$_2$(μ-C_5H_5)$_2$] (R = cyclo-C_6H_{11} (VIIa) or Pr^i (VIIb)). Only a trace of the compounds V were formed in these reactions. Data for the complexes VII are given in Tables 1 and 2, but the precise nature of these products was only established by an X-ray diffraction study on VIIb.

The results of the X-ray study are summarised in Table 5, and two views of the molecule, which has an approximate (non-crystallographic) two-fold axis of symmetry, are given in Figs. 4 and 5. The carbido ligand bridges the four metal atoms (Ru(1)–C 1.890(8), Ru(2)–C 1.903(8), Pt(1)–C 2.092(9), and Pt(2)–C 2.08(1) Å), but the Pt · · · Pt separation (3.132(1) Å) implies little or no direct metal–metal bonding. Carbonyl groups bridge the Ru(1)–Pt(1) and Ru(2)–Pt(2) connectivities. Potential energy minimisation calculations [22] indicated low energy hydride sites bridging the Ru(1)–Pt(2) and Ru(2)–Pt(1) vectors. The disposition of the carbido ligand is best revealed by Fig. 5, which emphasises the near linearity of the Ru(1)–C–Ru(2) (175.4(5)°) arrangement, and the non-planarity of the metal atoms. The angle between the Pt(1)Pt(2)Ru(1) and Pt(1)Pt(2)Ru(2) planes is 111°, and the P(1)Pt(1)Pt(2)P(2) torsion angle is 42.2°.

Table 5

Selected internuclear distances (Å) and angles (°) for $[Ru_2Pt_2(\mu\text{-}H)_2(\mu_4\text{-}C)(\mu\text{-}CO)_2(PPr^i_3)_2(\eta\text{-}C_5H_5)_2]$ (VIIb), with estimated standard deviations in parentheses

Pt(1)...Pt(2)	3.132(1)	Pt(1)–Ru(1)	2.707(1)
Pt(1)–Ru(2)	2.850(1)	Pt(1)–P(1)	2.264(3)
Pt(1)–C	2.092(9)	Pt(1)–C(1)	2.008(9)
Pt(2)–Ru(1)	2.858(1)	Pt(2)–Ru(2)	2.707(1)
Pt(2)–P(2)	2.272(3)	Pt(2)–C	2.08(1)
Pt(2)–C(2)	2.008(9)	Ru(1)–C	1.890(8)
Ru(1)–C(1)	2.06(1)	Ru(2)–C	1.903(8)
Ru(2)–C(2)	2.04(1)	C(1)–O(1)	1.18(1)
C(2)–O(2)	1.19(1)		
Pt(2)–Pt(1)–Ru(1)	58.1(1)	Pt(2)–Pt(1)–Ru(2)	53.6(1)
Ru(1)–Pt(1)–Ru(2)	85.9(1)	Pt(2)–Pt(1)–P(1)	137.1(1)
Ru(1)–Pt(1)–P(1)	149.6(1)	Ru(2)–Pt(1)–P(1)	124.4(1)
Pt(2)–Pt(1)–C	41.2(3)	Ru(1)–Pt(1)–C	44.1(2)
Ru(2)–Pt(1)–C	41.9(2)	P(1)–Pt(1)–C	166.3(2)
Pt(2)–Pt(1)–C(1)	90.4(3)	Ru(1)–Pt(1)–C	49.0(3)
Ru(2)–Pt(1)–C(1)	134.4(3)	P(1)–Pt(1)–C(1)	100.8(3)
C–Pt(1)–C(1)	92.9(4)	Pt(1)–Pt(2)–Ru(1)	53.5(1)
Pt(1)–Pt(2)–Ru(2)	57.9(1)	Ru(1)–Pt(2)–Ru(2)	85.8(1)
Pt(1)–Pt(2)–P(2)	141.4(1)	Ru(1)–Pt(2)–P(2)	125.4(1)
Ru(2)–Pt(2)–P(2)	148.5(1)	Pt(1)–Pt(2)–C	41.5(2)
Ru(1)–Pt(2)–C	41.3(2)	Ru(2)–Pt(2)–C	44.5(2)
P(2)–Pt(2)–C	165.8(2)	Pt(1)–Pt(2)–C(2)	88.2(3)
Ru(1)–Pt(2)–C(2)	133.2(3)	Ru(2)–Pt(2)–C(2)	48.4(3)
P(2)–Pt(2)–C(2)	101.2(3)	C–Pt(2)–C(2)	92.6(4)
Pt(1)–Ru(1)–Pt(2)	68.4(1)	Pt(1)–Ru(1)–C	50.4(3)
Pt(2)–Ru(1)–C	46.6(3)	Pt(1)–Ru(1)–C(1)	47.5(2)
Pt(2)–Ru(1)–C(1)	97.6(3)	C–Ru(1)–C(1)	97.7(4)
Pt(1)–Ru(2)–Pt(2)	68.6(1)	Pt(1)–Ru(2)–C	47.2(3)
Pt(2)–Ru(2)–C	50.0(3)	Pt(1)–Ru(2)–C(2)	95.9(3)
Pt(2)–Ru(2)–C(2)	47.5(2)	C–Ru(2)–C(2)	97.2(4)
Pt(1)–C–Pt(2)	97.4(4)	Pt(1)–C–Ru(1)	85.5(4)
Pt(2)–C–Ru(1)	92.0(3)	Pt(1)–C–Ru(2)	90.9(3)
Pt(2)–C–Ru(2)	85.5(4)	Ru(1)–C–Ru(2)	175.4(5)
Pt(1)–C(1)–Ru(1)	83.5(4)	Pt(1)–C(1)–O(1)	139.1(7)
Ru(1)–C(1)–O(1)	137.3(7)	Pt(2)–Ru(2)–C(2)	84.1(4)
Pt(2)–C(2)–O(2)	139.2(8)	Ru(2)–C(2)–O(2)	136.7(7)

Although folded along the Pt · · · Pt vector, the metal core of VIIb does not have a butterfly geometry in the usual sense as there is no discernible platinum–platinum bond (see above). In contrast, the 'mixed-metal' carbido clusters $[N(PPh_3)_2][Fe_3Rh(\mu_4\text{-}C)(CO)_{12}]$ and $[N(PPh_3)_2][Fe_3Mn(\mu_4\text{-}C)(CO)_{13}]$ [15b], and the homonuclear cluster $[Fe_4(\mu_4\text{-}C)(CO)_{13}]$ [23] have conventional butterfly configurations. It is also interesting to compare the structure of VIIb with that of compound I which has a 'spiked triangle' configuration for the metal core [9].

The spectroscopic data for VIIa and VIIb are completely consistent with the solid state structure established for the latter. In the IR spectrum of both species two bands are seen in the bridging carbonyl region (Table 1). The ^1H NMR spectra of VIIa and VIIb show high-field resonances for the μ-H ligands, each signal appearing as a doublet due to ^{31}P–^1H coupling (Table 2). Two sets of ^{195}Pt satellite peaks are

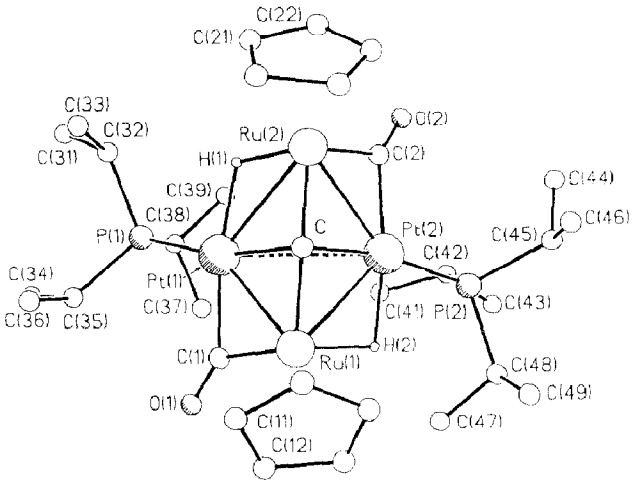

Fig. 4. The molecular structure of $[Ru_2Pt_2(\mu\text{-}H)_2(\mu_4\text{-}C)(\mu\text{-}CO)_2(PPr^i_3)_2(\eta\text{-}C_5H_5)_2]$ (VIIb) showing the crystallographic numbering scheme.

observed, with the stronger ^{195}Pt–^1H coupling (ca. 600 Hz) of magnitude comparable with the values found for similar coupling in the ^1H NMR spectra of the complexes VI. As a consequence of the two-fold symmetry of the compounds VII, the $Pt(PR_3)$ groups are equivalent, and hence only one ^{31}P and one ^{195}Pt resonance is observed in the NMR spectra of these nuclei. The ^{13}C-$\{^1H\}$ NMR spectra display peaks for the μ_4-C ligands at δ 438.9 (VIIa) and 439.5 ppm (VIIb). The spectrum of VIIb was of sufficient quality for the μ_4-C signal to be observed as a triplet (J(PC) 23 Hz) with one set of ^{195}Pt satellite peaks (J(PtC) 104 Hz).

The results described in this paper, and previously [9], illustrate a synthetic route to carbido-carbonyl metal clusters involving metal-promoted hydride removal from μ-methylene and μ-methylidyne ligands. Moreover, the reactions are clearly relevant to Fischer–Tropsch chemistry [24–26].

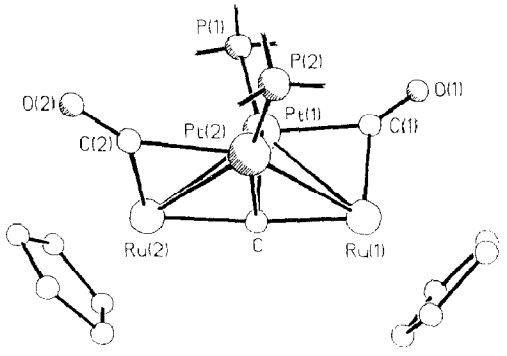

Fig. 5. Molecular structure of VIIb showing the geometry of the μ_4-CRu_2Pt_2 core. The Pr^i substituents on P(1) and P(2), and the hydrido ligands bridging Pt(1)–Ru(2) and Pt(2)–Ru(1) have been omitted for clarity.

Experimental

All experiments were carried out under nitrogen, using Schlenk tube techniques. Light petroleum refers to that fraction of b.p. 40–60 °C. The compounds $[Pt(cod)_2]$ [27], $[Pt(C_2H_4)_2(PR_3)]$ (R = cyclo-C_6H_{11} or Pr^i) [28], and $[Ru_2(\mu\text{-}CH_2)(\mu\text{-}CO)(CO)(L)(\eta\text{-}C_5H_5)_2]$ (L = CO or NCMe) [29] were obtained by methods previously described. Chromatography columns were of alumina (Brockman, Activity II). NMR spectra were measured with JEOL JNM FX90Q, GX270 and GX400 spectrometers. IR spectra were recorded with Nicolet 10-MX and 5Z-DX spectrophotometers.

Synthesis of the ruthenium-platinum complexes

(i) A cold (0 °C) ethylene-saturated light petroleum (50 cm^3) solution of $[Pt(C_2H_4)_2\{P(C_6H_{11})_3\}]$ (3.24 mmol) was prepared in situ from $[Pt(cod)_2]$ (1.33 g, 3.24 mmol), and $P(C_6H_{11})_3$ (0.91 g, 3.24 mmol) [28]. The solution was transferred (ethylene pressure) via a flexible steel cannula to a Schlenk tube containing IVa (0.70 g, 1.62 mmol). Solvent was removed in vacuo and replaced by Et_2O (40 cm^3), and the mixture ws stirred for 30 h at room temperature. Solvent was removed in vacuo, and the residue was dissolved in light petroleum (ca. 15 cm^3) and chromatographed (2.5 × 20 cm column). Elution with light petroleum/CH_2Cl_2 (5 : 1) gave a purple fraction which after removal of solvent in vacuo yielded purple crystals of $[Ru_2Pt(\mu\text{-}CH_2)(\mu\text{-}CO)(CO)_2\{P(C_6H_{11})_3\}(\eta\text{-}C_5H_5)_2]$ (Va) (1.01 g). Further elution of the column with light petroleum/CH_2Cl_2 (1/1) separated two yellow bands. The first to be eluted contained unreacted IVa, while the second, following removal of solvent in vacuo, afforded yellow-orange crystals of $[Ru_2Pt_2(\mu\text{-}H)(\mu_4\text{-}CH)(\mu\text{-}CO)(CO)_2\{P(C_6H_{11})_3\}_2(\eta\text{-}C_5H_5)_2]$ (VIa) (0.11 g).

(ii) In a similar procedure, $[Pt(C_2H_4)_2(PPr^i_3)]$ (1.09 mmol) and IVa (0.23 g, 0.054 mmol) in Et_2O (30 cm^3), after stirring for ca. 30 h at room temperature, gave purple crystals of $[Ru_2Pt(\mu\text{-}CH_2)(\mu\text{-}CO)(CO)_2(PPr^i_3)(\eta\text{-}C_5H_5)_2]$ (Vb) (0.29 g) and yellow crystals of $[Ru_2Pt_2(\mu\text{-}H)(\mu_4\text{-}CH)(\mu\text{-}CO)(CO)_2(PPr^i_3)_2(\eta\text{-}C_5H_5)_2]$ (VIb) (0.048 g).

(iii) A cold (0 °C) ethylene-saturated light petroleum (50 cm^3) solution of $[Pt(C_2H_4)_2\{P(C_6H_{11})_3\}]$ (1.12 mmol) was prepared from $[Pt(cod)_2]$ (0.46 g, 1.12 mmol) and $P(C_6H_{11})_3$ (0.32 g, 1.12 mmol), and transferred to a Schlenk tube containing IVb (0.26 g, 0.56 mmol). Solvent was removed in vacuo, and the residue was dissolved in Et_2O (40 cm^3). The suspension was stirred for 48 h at room temperature. Solvent was removed in vacuo, and the residue was dissolved in light petroleum (ca. 20 cm^3) and chromatographed. Elution with light petroleum/CH_2Cl_2 (5 : 1) removed a trace of purple Va. Further elution with light petroleum/CH_2Cl_2 (2 : 1) separated two yellow fractions. The first to be eluted gave, after removal of solvent in vacuo, yellow crystals of $[Ru_2Pt_2(\mu\text{-}H)_2(\mu_4\text{-}C)(\mu\text{-}CO)_2\{P(C_6H_{11})_3\}_2(\eta\text{-}C_5H_5)_2]$ (VIIa) (0.34 g). The second yellow eluate afforded, after removal of solvent, yellow orange crystals of VIa (0.62 g).

(iv) In a similar manner, the reaction between $[Pt(C_2H_4)_2(PPr^i_3)]$ (1.09 mmol) and IVb (0.23 g, 0.54 mmol) gave a trace of Vb, and the compounds $[Ru_2Pt_2(\mu\text{-}H)_2(\mu_4\text{-}C)(\mu\text{-}CO)_2(PPr^i_3)_2(\eta\text{-}C_5H_5)_2]$ (VIIb) (0.25 g) and VIb (0.037 g).

Crystal structure determinations

Data were collected using Nicolet $P2_1$ or P3 diffractometers (293 K, Mo-K_α X-radiation, graphite monochromator, $\bar{\lambda}$ 0.71069 Å). The data were corrected for

Lorentz, polarisation and X-ray absorption effects. The structures were solved by conventional heavy atom or direct methods, and successive difference Fourier syntheses were used to locate all non-hydrogen atoms. Final refinements by blocked-cascade least squares were performed on a Data General 'Eclipse' computer with the SHELXTL system of programs [30]. Scattering factors with corrections for

Table 6

Atomic positional parameters (fractional coordinates $\times 10^4$) for compound Va with estimated standard deviations in parentheses

Atom	x	y	z
Pt	3577(1)	2201(1)	2557(1)
Ru(1)	5894(1)	2951(1)	2282(1)
Ru(2)	4007(1)	3147(1)	1114(1)
P	2256(2)	1191(2)	3389(2)
C(1)	5168(9)	2003(10)	3216(7)
C(2)	2272(10)	2684(10)	1868(8)
O(2)	1124(8)	2781(9)	1784(7)
C(3)	6538(10)	1662(10)	1377(8)
O(3)	7026(9)	800(8)	827(7)
C(4)	3469(11)	4570(10)	1908(8)
O(4)	3089(9)	5481(7)	2355(7)
C(11)	6256(11)	4790(8)	2371(8)
C(12)	7495	4078	2046
C(13)	7711	3572	2800
C(14)	6606	3972	3591
C(15)	5707	4725	3326
C(21)	3497(15)	3341(13)	−277(7)
C(22)	3313	2233	−216
C(23)	4578	1667	−216
C(24)	5543	2425	−276
C(25)	4875	3460	−314
C(31)	920(8)	659(8)	2772(6)
C(32)	1412(10)	−102(10)	1755(7)
C(33)	236(12)	−283(12)	1233(8)
C(34)	−893(12)	−733(12)	1811(10)
C(35)	−1350(11)	3(11)	2830(9)
C(36)	−190(10)	189(10)	3344(8)
C(41)	3245(8)	35(7)	3667(6)
C(42)	2517(10)	−625(10)	4318(8)
C(43)	3507(11)	−1390(10)	4611(9)
C(44)	4433(12)	−2188(9)	3735(9)
C(45)	5122(11)	−1541(10)	3083(8)
C(46)	4154(11)	−766(9)	2775(7)
C(51)	1329(9)	2036(8)	4587(6)
C(52)	345(11)	2981(9)	4516(7)
C(53)	−453(11)	3649(10)	5508(8)
C(54)	472(12)	4099(10)	6170(8)
C(55)	1464(11)	3174(11)	6255(7)
C(56)	2249(10)	2497(9)	5265(7)
O(60)	0	5000	0
C(60)	−885(28)	3738(23)	−1062(16)
C(61)	−281(33)	4364(32)	−625(32)

Table 7

Atomic positional parameters (fractional coordinates $\times 10^4$) for compound VIb with estimated standard deviations in parentheses

Atom	x	y	z
Pt(1)	1670(1)	1613(1)	2434(1)
Pt(2)	3369(1)	2750(1)	2925(1)
Ru(1)	3279(1)	3273(1)	1584(1)
Ru(2)	1881(1)	1795(1)	1129(1)
P(1)	698(2)	520(2)	2673(1)
P(2)	4899(2)	3089(2)	3917(1)
C(1)	2074(8)	2709(6)	1896(5)
C(2)	2509(8)	2068(6)	3415(5)
O(2)	2514(6)	1977(5)	3974(4)
C(3)	2896(11)	977(7)	1699(7)
O(3)	3521(8)	432(6)	2003(6)
C(4)	4047(15)	2315(9)	1463(10)
O(4)	4722(11)	1869(7)	1383(9)
C(11)	2261(14)	4339(10)	870(10)
C(12)	2992(16)	4027(9)	616(7)
C(13)	4032(14)	4231(10)	1074(11)
C(14)	3912(15)	4638(8)	1647(8)
C(15)	2826(16)	4706(8)	1519(9)
C(21)	1182(11)	2013(9)	−52(6)
C(22)	442(13)	2380(11)	225(7)
C(23)	45(12)	1674(15)	524(8)
C(24)	561(15)	928(12)	437(7)
C(25)	1267(12)	1117(9)	67(6)
C(31)	2667(11)	−283(9)	3617(8)
C(32)	1493(11)	29(7)	3543(6)
C(33)	871(15)	−696(11)	3801(8)
C(34)	−416(12)	1540(8)	3359(8)
C(35)	−631(9)	907(7)	2722(7)
C(36)	−1371(11)	1338(11)	2020(9)
C(37)	−686(11)	−1000(8)	2031(8)
C(38)	191(10)	−351(7)	1978(7)
C(39)	1135(11)	−840(8)	1896(8)
C(41)	6174(11)	2530(8)	5364(6)
C(42)	5222(9)	2287(7)	4654(5)
C(43)	5352(13)	1368(7)	4424(7)
C(44)	6539(14)	2523(10)	3449(11)
C(45)	6185(9)	3304(7)	3727(7)
C(46)	7163(10)	3774(12)	4321(7)
C(47)	3683(10)	4012(8)	4557(7)
C(48)	4632(8)	4131(6)	4295(5)
C(49)	4347(12)	4848(7)	3747(7)

anomalous dispersion were taken from ref. 31. Atom coordinates are given in Tables 6–8.

Full listings of bond distances and angles, and thermal parameters have been deposited with the Cambridge Crystallographic Data Centre, University Chemical Laboratory, Lensfield Road, Cambridge CB2 1EW. Structure factors are available from the authors.

Table 8

Atomic positional parameters (fractional coordinates $\times 10^4$) for compound VIIb with estimated standard deviations in parentheses

Atom	x	y	z
Pt(1)	3701(1)	3804(1)	2340(1)
Pt(2)	3715(1)	1673(1)	1797(1)
Ru(1)	6058(1)	2079(1)	2345(1)
Ru(2)	3062(1)	3608(1)	446(1)
P(1)	2322(3)	5069(2)	3102(2)
P(2)	3269(3)	128(2)	2427(2)
C	4615(9)	2838(7)	1358(6)
C(1)	5188(10)	2898(8)	3403(7)
O(1)	5477(8)	2866(6)	4222(5)
C(2)	2006(10)	2602(8)	928(7)
O(2)	909(7)	2588(7)	749(7)
C(11)	8055(10)	2330(10)	2370(8)
C(12)	8081(10)	1534(10)	3254(8)
C(13)	7974(11)	632(10)	2988(9)
C(14)	7903(10)	846(10)	1937(9)
C(15)	7975(12)	1864(11)	1580(8)
C(21)	2043(12)	5210(10)	−658(7)
C(22)	1484(12)	4525(10)	−867(7)
C(23)	2516(13)	3634(10)	−1073(7)
C(24)	3787(13)	3755(11)	−1044(7)
C(25)	3459(13)	4782(10)	−788(7)
C(31)	52(14)	7184(10)	2606(9)
C(32)	1170(10)	6300(8)	2205(7)
C(33)	1905(14)	6809(10)	1392(8)
C(34)	2418(14)	6115(11)	4653(10)
C(35)	3266(11)	5437(8)	3962(7)
C(36)	4283(14)	5921(11)	3465(10)
C(37)	1901(13)	3555(9)	4691(7)
C(38)	1128(11)	4573(8)	3876(7)
C(39)	172(12)	4305(10)	3249(8)
C(41)	1695(15)	1128(11)	3853(9)
C(42)	1765(10)	350(8)	3197(7)
C(43)	1617(12)	−712(9)	3782(8)
C(44)	1344(12)	−116(11)	1179(9)
C(45)	2864(11)	−523(9)	1502(7)
C(46)	3736(15)	−407(11)	610(9)
C(47)	5065(12)	−736(10)	4111(8)
C(48)	4684(11)	−1028(8)	3209(7)
C(49)	5957(12)	−1392(11)	2627(11)

Structure determination of $[Ru_2Pt(\mu\text{-}CH_2)(\mu\text{-}CO)(CO)_2\{P(C_6H_{11})_3\}(\eta\text{-}C_5H_5)_2]$ *(Va)*

Crystals of Va were grown from diethyl ether at −20 °C as black parallelepipeds (crystal dimensions ca. 0.02 × 0.15 × 0.08 mm). Of the 5846 data collected (θ–2θ scans, $2\theta \leq 50°$, weak reflections were not collected for $2\theta \geq 40°$), 4150 unique data had $F \geq 4\sigma(F)$, and only these were used for structure solution and refinement. An empirical absorption correction was applied using a method based upon azimuthal scan data.

Crystal data for Va. $C_{32}H_{45}O_3PPtRu_2 \cdot \frac{1}{2}(C_4H_{10}O)$, $M = 943.0$, triclinic, space group $P\bar{1}$, a 10.215(4), b 12.381(4), c 14.484(4) Å, α 103.54(3), β 79.74(3), γ

85.44(3)°, U 1738(1) Å^3, $Z = 2$, D_c 1.80 g cm^{-3}, $F(000) = 926$, μ(Mo-K_α) 49.8 cm^{-1}.

The asymmetric unit contains half a molecule of diethyl ether, the oxygen atom of which lies at (0, 0.5, 0). All non-hydrogen atoms were refined with anisotropic thermal parameters. All non-solvent hydrogen atoms were included in calculated positions (C–H 0.96 Å) with fixed isotropic thermal parameters ca. $1.2 \times U_{equiv.}$ of the parent carbon atoms. The cyclopentadienyl ring systems were treated as rigid groups (C–C 1.42 Å). Final $R = 0.041$ ($R' = 0.038$) with a weighting scheme of the form $w^{-1} = [\sigma^2(F) + 0.00034 \mid F \mid^2]$. The final electron density difference synthesis showed no peaks > 1.10 or < -0.76 eÅ^{-3}.

Structure determination of $[Ru_2Pt_2(\mu\text{-}H)(\mu_4\text{-}CH)(\mu\text{-}CO)(CO)_2(PPr^i_3)_2(\eta\text{-}C_5H_5)_2]$ *(VIb)*

Crystals of VIb were grown from dichloromethane/light petroleum mixtures as orange plates (crystal dimensions ca. $0.075 \times 0.14 \times 0.18$ mm with well developed faces of the types (0, 0, 1), (0, 0, $\bar{1}$), (1, $\bar{1}$, 0), ($\bar{1}$, 1, 0), (1, 1, 0), ($\bar{1}$, $\bar{1}$, 0)). Of the 7411 data collected (θ–2θ scans, $2\theta \leqslant 50°$), 5122 unique data had $F \geqslant 4\sigma(F)$, and only these were used for structure solution and refinement. The data were corrected for X-ray absorption effects by an analytical method using crystal faces.

Crystal data for VIb. $C_{32}H_{54}O_3P_2Pt_2Ru_2$, $M = 1141.1$, monoclinic, space group $P2_1/c$, a 12.833(2), b 15.270(2), c 20.486(4) Å, β 112.71(1)°, U 3703(1) Å^3, $Z = 4$, D_c 2.05 g cm^{-3}, $F(000) = 2176$, μ(Mo-K_α) 85.1 cm^{-1}.

All non-hydrogen atoms were refined with anisotropic thermal parameters. The μ-H and μ_4-CH hydrogen atoms were located in a final difference map and were refined with fixed isotropic thermal parameters of 0.05 and 0.038 Å^2 respectively. The refined μ-H position agreed well with the results of a potential energy minimisation calculation [22]. All other hydrogen atoms were included in calculated positions (C–H 0.96 Å) with either fixed isotropic thermal parameters ca. $1.2 \times U_{equiv.}$ of the parent carbon atoms (C*H*Me$_2$ and η-C$_5$H$_5$), or a common refined isotropic thermal parameter (CH*Me*$_2$). Final $R = 0.041$ ($R' = 0.038$) with a weighting scheme of the form $w^{-1} = [\sigma^2(F) + 0.00046 \mid F \mid^2]$. The final electron density difference synthesis showed no peaks > 1.6 or < -1.4 eÅ^{-3}.

Structure determination of $[Ru_2Pt_2(\mu\text{-}H)_2(\mu_4\text{-}C)(\mu\text{-}CO)_2(PPr^i_3)_2(\eta\text{-}C_5H_5)_2]$ *(VIIb)*

Crystals of VIIb were grown from dichloromethane/light petroleum mixtures as orange plates (crystal dimensions ca. $0.40 \times 0.15 \times 0.25$ mm). Of the 4377 data collected (Wyckoff ω-scans, $2\theta \leqslant 42°$), 3282 unique data had $F \geqslant 4\sigma(F)$, and only these were used for structure solution and refinement. The data were corrected for X-ray absorption effects by an empirical method based upon azimuthal scan data.

Crystal data for VIIb. $C_{31}H_{54}O_2P_2Pt_2Ru_2$, $M = 1113.0$, triclinic, space group $P\bar{1}$, a 10.471(2), b 13.476(3), c 14.038(4) Å, α 76.51(2), β 88.56(2), γ 68.74(2)°, U 1791(1) Å^3, $Z = 2$, D_c 2.06 g cm^{-3}, $F(000) = 1060$, μ(Mo-K_α) 87.9 cm^{-1}.

All non-hydrogen atoms were refined with anisotropic thermal parameters. The μ-H hydrogen atom positions shown in Fig. 4 were determined using a potential energy minimisation program [22], but these atoms were not included in the refinement (calculated coordinates: H(1) 0.229, 0.441, 0.136; H(2) 0.537, 0.097, 0.253; Pt–H and Ru–H separations of ca. 1.85 Å were used in the calculations). All other hydrogen atoms were included in calculated positions (C–H 0.96 Å) with

either fixed isotropic thermal parameters ca. $1.2 \times U_{equiv.}$ of the parent carbon atoms ($CH\mathrm{Me}_2$ and η-C_5H_5), or a common refined isotropic thermal parameter ($CH\mathrm{Me}_2$). Final $R = 0.029$ ($R' = 0.029$) with a weighting scheme of the form $w^{-1} = [\sigma^2(F) + 0.00045|F|^2]$. The final electron density difference synthesis showed no peaks > 0.93 or -0.83 eÅ^{-3}

Acknowledgements

We thank U.K. SERC for support.

References

1 F.G.A. Stone, Acc. Chem. Res., 23 (1984) 89; and ref. cited therein.
2 F.G.A. Stone, Inorg. Chim. Acta, 50 (1981) 33.
3 (a) L.J. Farrugia, J.A.K. Howard, P. Mitrprachachon, F.G.A. Stone, and P. Woodward, J. Chem. Soc., Dalton Trans., (1981) 155; (b) idem., ibid., (1981) 1134; (c) idem., ibid., (1981) 1274.
4 L.J. Farrugia and P. Mitrprachachon, Ph.D. Theses, Bristol University, 1979.
5 M. Green, J.A.K. Howard, G.N. Pain, F.G.A. Stone, J. Chem. Soc., Dalton Trans., (1982) 1327.
6 M.J. Freeman, A.D. Miles, M. Murray, A.G. Orpen, and F.G.A. Stone, Polyhedron, 3 (1984) 1093.
7 G.P. Elliot, J.A.K. Howard, T. Mise, C.M. Nunn, and F.G.A. Stone, J. Chem. Soc., Dalton Trans., (1987) 2189.
8 L.J. Farrugia, J.A.K. Howard, P. Mitrprachachon, J.L. Spencer, F.G.A Stone, and P. Woodward, J. Chem. Soc., Chem. Commun., (1978) 260.
9 L.J. Farrugia, A.D. Miles, and F.G.A. Stone, J. Chem. Soc., Dalton Trans., (1985) 2437.
10 J.S. Bradley, Adv. Organomet. Chem., 22 (1983) 1.
11 M. Tachikawa and E.L. Muetterties, Prog. Inorg. Chem., 28 (1981) 203.
12 E.H. Braye, L.F. Dahl, W. Hubel, and D.L. Wampler, J. Am. Chem. Soc., 84 (1962) 4633.
13 M. Tachikawa, A.C. Sievert, E.L. Muetterties, M.R. Thompson, C.S. Day, and V.W. Day, J. Am. Chem. Soc., 102 (1980) 1725.
14 J.S. Bradley, R.L. Pruett, E. Hill, G.B. Ansell, M.E. Leonowicz, and M.A. Modrick, Organometallics, 1 (1982) 748.
15 (a) J.W. Kolis, E.M. Holt, J.A. Hriljac, and D.F. Shriver, Organometallics, 3 (1984) 496; (b) J.A. Hriljac, P.N. Swepston, and D.F. Shriver, ibid., 4 (1985) 158; (c) J.A. Hriljac, E.M. Holt, and D.F. Shriver, Inorg. Chem., 26 (1987) 2943; (d) P.L. Stanghellini, M.J. Sailor, P. Kuznesof, K.H. Whitmire, J.A. Hriljac, J.W. Kolis, Y. Zheng, and D.F. Shriver, ibid., 26 (1987) 2950.
16 D.L. Davies, J.C. Jeffery, D. Miguel, P. Sherwood, and F.G.A. Stone, J. Chem. Soc., Chem. Commun., (1987) 454.
17 N. Cook, L.E. Smart, P. Woodward, and J.D. Cotton, J. Chem. Soc., Dalton Trans., (1979) 1032.
18 R.E. Colborn, D.L. Davies, A.F. Dyke, A. Endesfelder, S.A.R. Knox, A.G. Orpen, and D. Plaas, J. Chem. Soc. Dalton Trans., (1983) 2661; and ref. cited therein.
19 A. Modinos and P. Woodward, J. Chem. Soc., Dalton Trans., (1975) 1534.
20 M.I. Bruce, J.G. Matisons, B.W. Skelton, and A.H. White, Aust. J. Chem., 35 (1982) 687.
21 M.A. Beno, J.M. Williams, M. Tachikawa, and E.L. Muetterties, J. Am. Chem. Soc., 103 (1981) 1485.
22 A.G. Orpen, J. Chem. Soc., Dalton Trans., (1980) 2509.
23 J.S. Bradley, G.B. Ansell, M.E. Leonowicz, and E.W. Hill, J. Am. Chem. Soc., 103 (1981) 4968.
24 R.B. Anderson, The Fischer-Tropsch Synthesis, Academic Press, London, 1984.
25 G. Henrici-Olivé and S. Olivé, Angew. Chem. Int. Ed. Engl., 15 (1976) 136.
26 R.P.A. Sneedon in E.W. Abel, F.G.A. Stone, and G. Wilkinson (Eds.): Comprehensive Organometallic Chemistry, Pergamon Press, N.Y. 1982, Vol. 8, p. 40–73.
27 J.L. Spencer, Inorg. Synth., 19 (1979) 213.
28 N.C. Harrison, M. Murray, J.L. Spencer, and F.G.A. Stone, J. Chem. Soc., Dalton Trans., (1978) 1337; J.C. Jeffery, M.A. Ruiz, and F.G.A. Stone, J. Organomet. Chem., 355 (1988) 231.
29 D.L. Davies, S.A.R. Knox, K.A. Mead, M.J. Morris, and P. Woodward, J. Chem. Soc., Dalton Trans., (1984) 2293; N.M. Doherty, J.A.K. Howard, S.A.R. Knox, and N.J. Terrill, J. Chem. Soc., Chem. Commun., (1989) 638.
30 G.M. Sheldrick, SHELXTL programs for use with the Nicolet X-ray system, Revision 5.1, 1986.
31 'International Tables for X-Ray Crystallography', Kynoch Press, Birmingham, 1974, Vol. 4.